Direct Classic Route of Generating Mono-Color EM-Pulse with Attosecond-Level Duration

Hai Lin * and **Chengpu Liu**

Shanghai Institute of Optics and Fine Mechanics, CAS, Shanghai 201800, China; chpliu@siom.ac.cn

* Correspondence: linhai@siom.ac.cn; Tel.: +86-21-6991-8266

check for updates

Abstract: Current conception of attosecond pulse is based on Fourier optics and refers to an electromagnetic pulse with a broad, homogeneous weight Fourier spectrum. Its preparation/generation is along an indirect route in which the output of commercial available μm-level wavelength laser is "processed" by elaborately designed optics medium allowing high-order harmonics effect to change its Fourier spectrum to be of a flat high-frequency tail. Such an indirect, quantum scheme is limited by its efficiency in high-order harmonics generation. For higher efficiency, other routes for the same goal, i.e., light pulse with an attosecond-level duration, deserve to be tried. The method proposed is a direct, classic scheme. It is to directly control the time duration of classic electrons doing acceleration/deceleration in a feasible, elaborately-designed driving DC fields configuration. The duration can be adjusted by initial electrons velocity, geometric dimension of driving field configuration. The maximum strength of a generated pulse is controlled by the number of electrons. The frequency of a generated pulse is controlled by initial electrons position in the configuration. The shortest duration of single pulse can be down to sub-attosecond-level according to currently available minimum geometric dimension of driving field and suitable gesture of electrons entering into the driving field configuration. This work displays a feasible, direct, classic route of achieving EM pulse with an attosecond-level duration. In particular, the pulse is mono-color, rather than a superposition of Fourier components with nearly-equal weight.

Keywords: attosecond; laser pulse; radiation source; attosecond duration; classic orbit

1. Introduction

Demands from applications promote the progress in preparing/generating ultrashort-duration, down to wavelength-level or shorter, laser pulse [1–10], which in turn promotes new applications areas appearing [11–20]. For applications emphasizing high energy density, spectral broadening technique, which relies on optical property of bulk material [21–24] and fine adjusting optical elements [25–27], can supply single μm-level wavelength laser pulse with femtosecond(fs)-level duration and mJ-level energy. For applications emphasizing optics probing and optical manipulation of quantum system, the pulse is not required to be high-energy-density but to be of a shorter duration down to attosecond(as)-level. Current technique routes for achieving as-level duration are from (1) high-order harmonics generation (HHG) from laser-irradiated atoms in gaseous medium [1–4,28–33]. (2) HHG effect in laser–plasma interaction [34,35]. (3) The interaction between laser and electron beam free-electron-laser (FEL) facility [36–38]. In these routes, Fourier components with shorter wavelength (below half of incident central wavelength) are produced from the interaction of the incident pulse with matter mentioned above. The ability of the pulse being shortened is determined by the efficiency of producing these Fourier components.

All these routes face the same difficulty, the efficiency. In the laser–atom route, the amplitude of higher-order harmonic component decreases exponentially with respect to the order.

For example, the intensity of 50-order component is 10^{-12} of that of the fundamental component [39]. Merely enhancing the intensity of the fundamental component is of little effect on this fact because the laser–atom route demands the survival of the involved quantum system, which does not favor the application of more intense fundamental components. The other two routes are based on the interaction of the fundamental component with classic electrons. Besides preparing plasmas, manipulating bulk plasma electrons to do a collective oscillation with a frequency multiple folds of the incident laser also demands the incident laser to be high-energy-density enough. The route based on FEL facility is also not optimistic in the efficiency because its background physics is associated with high-energy relativistic electrons and large-sized undulator magnetic field configuration, which are rather expensive for most university-level small research groups.

The commonality of these routes is to use easily-prepared electromagnetic (EM) Fourier components, such as visible and near-infrared laser with μm-level wavelength (from 1 μm to 0.4 μm), as "raw material" to produce, through different technique routes, EM Fourier components with wavelength <0.1 μm, which act as building components of desired pulse with as-level duration. Namely, producing the EM pulse with as-level duration is along an indirect way through the EM pulse with longer duration, or first producing a EM pulse with longer duration and then producing a EM pulse with as-level duration from this longer duration "raw material" supplied by a commercial available laser.

It is instructive and interesting to consider initially directly producing such a desired EM pulse with as-level duration. Retrospecting the history of laser, as well as its elder brother maser, we can find that the generation of EM pulse at visible and near-infrared band starts from flexible utilization of AC electric and magnetic field at power frequency (about tens Hz). A laser apparatus, due to electron structure of its kernel components/elements (i.e., gain medium), can convert power frequency input to optics-frequency output. The shortage of available material with electron structure suitable to 100 eV-level, or a level of tens nanometer (nm), wavelength optics output determines little hope, at least currently, of setting up a solid-state laser-like apparatus directly converting power frequency input to intense X-ray output. Of course, obtaining the as-level duration through plasma-based coherent X-ray source is obviously an expensive route.

However, if not being bound to suitable gain medium, we can try to consider the generation of radiation from low-energy electrons bunch in vacuum. The motive to this direction is for minimizing the dependence of generating radiations on kernel materials. Therefore, flexible usage of solid-state vacuum electron components/elements which are common in accelerator physics is the core of the technique route we consider.

Matured techniques in accelerator physics enables us to set up various configurations of DC magnetic field and DC electric field. These targeted designed field configurations can interact with incident electrons bunch to generate radiation. Many examples, such as FEL and synchronized radiation, have illustrated this point well. In FEL, a laser, or a EM optical-frequency, still need to be input and the incident electrons bunch is required to be sufficiently high-velocity. In contrast, the route presented in this work does not have these requirements.

The purpose is to seek for a cheap route of preparing EM pulse with as-level duration through the interaction of low-energy electrons bunch with targeted designed configuration of DC magnetic and electric fields. Based on previous works [40,41], it is feasible to achieve this goal because there is no severe requirement on components/elements. All components/elements are common in vacuum electron devices and working voltage and current are also low enough. The crucial part of this route is its idea, purposely preparing "defected" field configurations which can make electrons oscillate at desired frequency during a desired time scale. In the following sections, we will display details of this route.

2. Methods

The physics basis of our method can be summarized as "tailoring" Takeuchi-orbit. As shown in Takeuchi's theory [42], a single-electron orbit in an $E_s \perp B_s$ configuration, where E_s and B_s are both DC, can be divided into two classes: elliptical and hyperbola, according to initial velocity of the electron entering into the configuration and values of (E_s, B_s) [42,43]. The elliptical orbit implies that the electron does a time-periodic motion, or oscillation, along a "large" orbit and hence could potentially act as a radiation source. Therefore, for practical purposes, we propose to compress/tailor the geometric size of such a Takeuchi-orbit to a small-enough level by flexible utilization of various *DC*-field components/elements [40].

DC-field components/elements we used are very common. For example, Helmholtz coil pair is a common basic component for screening an external magnetic field. We let its two coils be not co-axial on purpose and hence make the magnetic field between them to be of a "defect" or a discontinuity in energy density profile B_s^2 [41]. More exactly, the phrase "discontinuity" should be replaced by "slope" because of realistic finite-sized components [40]. A pair of parallel metal-plates supplies a medium strength E_s vertical to B_s, and incident electrons, whose velocities are as slow as possible, are along the $E_s \times B_s$ direction and enter into the configuration from a position near the midpoint of the "slope" [40]. The E_s-field can be designed to be of a finite thickness, denoted as *Th* in Figure 1, in the incident direction of electrons bunch by applying high-dielectric-constant insulator medium to "mask" the metal plates (see Figure 1a). Thus, during the bunch crossing the $E_s \times B_s$, the electron bunch will oscillate along a "spliced" Takeuchi-orbit and the time-duration of doing such an oscillation can be handily controlled by adjusting the *Th*-value if initial incident electron velocity is given.

In such a configuration, the transverse aspect of the single-electron dynamics can be strictly controlled, through values of several parameters, to be an oscillation over the finite-sized "spliced" orbit [40,41]. The time cycle, or the frequency, of the oscillation can be controlled by values of those parameters and is, in principle, able to be arbitrary. Thus, relative to a far-field observer on the way of the electrons bunch, there is a mono-color light source. The magnitudes of E_s and B_s are not required to be high because one can adjust *D*-value to control the time cycle of the tailored Takeuchi-orbit [40,41]. To some extent, the tailoring Takeuchi-orbit scheme above-described is alike to well-known synchronization radiation apparatus being stretched to a straight-line by applying a $E_s \perp B_s$.

The time-duration of electrons travelling in such a configuration, which depends on the *Th*-value and incident longitudinal velocity of the bunch, determines the time-duration of electrons doing transverse oscillation. Besides adjusting the area of the parallel metal-plates, adjusting the relative position, (represented by *D* in Figure 1) and "gesture" of the plates to the midpoint of the slope, or the $B_s = 0$ contour, is also effective. As shown in Figure 1b, infinitely short time-duration is in principle able to be achieved.

However, realistic factors, such as available mechanics processing skill, determine the minimum time-duration to be large than a threshold. Currently available mechanics process skill can warrant μm-level positioning accuracy. For achieving *as*-level time-duration, nm-level positioning accuracy should be warranted. This can be achieved either through corresponding mechanics device in scanning electron microscope (SEM) or through simple component/element which can minify, according to "lever" principle (see Figure 2), the space step.
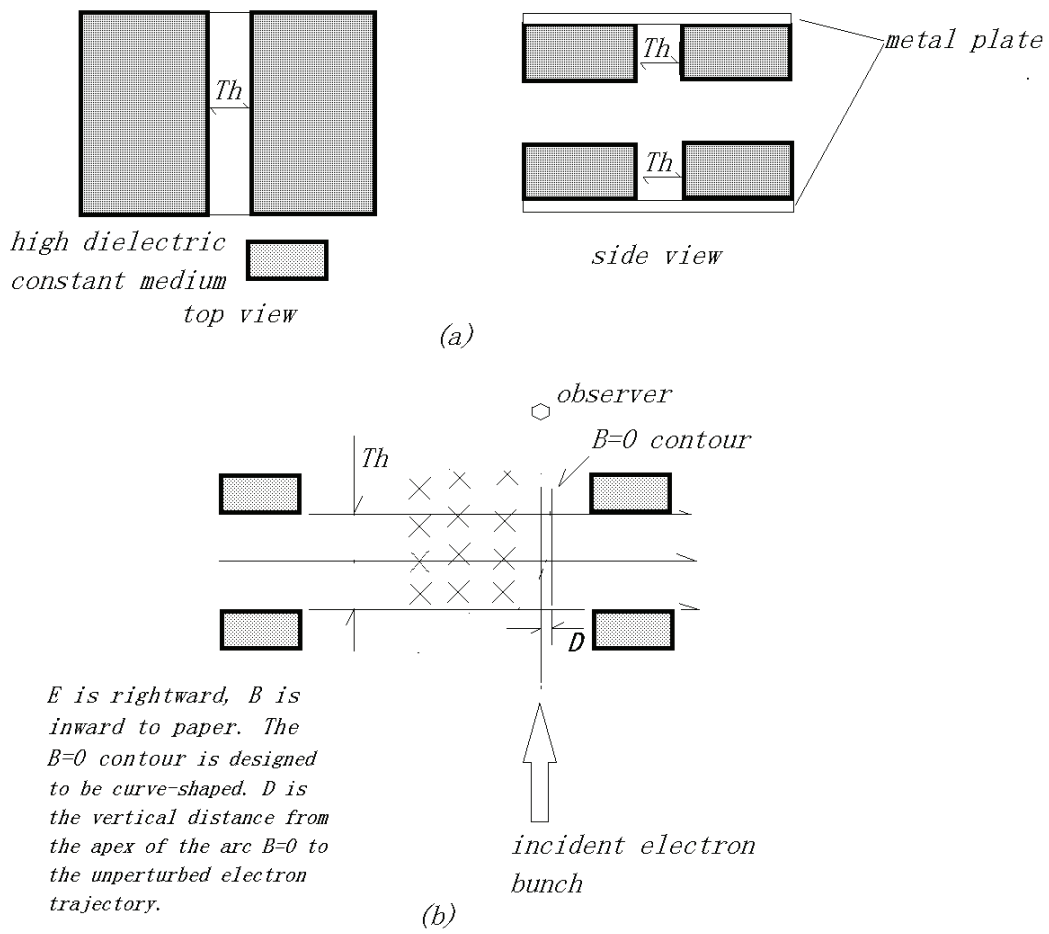
Figure 1. Sketch of field configuration (**a**) and experimental setup (**b**).
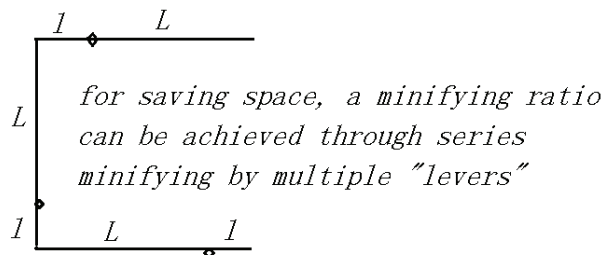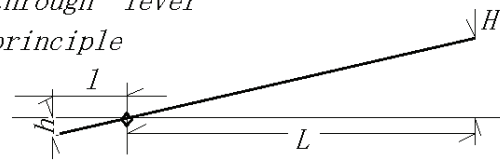

Figure 2. Sketch of the device for minifying space step.

A practical radiation source should have an obvious output power. Therefore, the charge of the bunch, or the number of electrons in the bunch, cannot be too low. The charge is dependent on the density of the parent material which supplies electrons. Considering the fact that the density of solid-state cathode is usually at 10^{22} cm^{-3} $= 10^{10}$ μm^{-3}-level, we should apply more realistic multiple-body dynamics method to this question.

Simulating up to 10^{12} or more electrons is a challenge. If each electron is described by 6 double-precision format (real-valued digit) floating-point numbers for its 3 space position coordinate components and 3 velocity components, 6×10^{12} double-precision format (real-valued digit) floating-point numbers needs up to 6×24 TB storage mount (i.e., a double-precision format (real-valued digit) floating-point numbers needs 24 Byte storage mount). Currently popular multiple-body dynamics methods, such as Particle-in-Cell simulation [44,45], are mostly in an exhaustive manner to simulate electrons. Because 6×24 TB storage mount is beyond the volume of faster semiconductor storage medium (i.e., memory) in computer groups and hence the simulation inevitably involves in time-consuming Input/Output (I/O) operation, which reads/writes data on slower magnetic harddisk (whose access time is usually at 0.5 GB per second-level), people have to invent approximation for speeding up the simulation at the cost of scientific reliability. For example, the PIC method usually contains two approximations, one is rigid-macroparticle approximation (RMPA) [46], and the other is alternative-updation approximation (AUA) [44,45]. Even though the number of electrons is so low, such as <10, that the RMPA is not hired, the AUA still threats the scientific reliability of the simulation.

This is because the PIC method is to solve a coupled set of N relativistic Newton equations (RNEs) and four Maxwell equations (MEs). As pointed out elsewhere [46], at any time t, although self-consistent electric field E can be known from all particles' information at the time t through a ME $\nabla \cdot E(r,t) = \sum_{i=1}^{N} \delta(r - r_i(t))$, self-consistent magnetic field B cannot. Due to the term $\partial_t E$ in the ME $\partial_t E - e \sum_{i=1}^{N} d_t r_i \delta(r - r_i(t)) = \nabla \times B$, the information of B at t has dependence on all particles' information at $t + \Delta t$. This implies that each difference version of RNE involves indeed all particles' coordinates at $t + \Delta t$, i.e., $\{r_i(t + \Delta t); 1 \leq i \leq N\}$ or

$$r_m([i+1]\Delta t) = F\left(\{r_{n \neq m}\}|_{t=[i+1]\Delta t}, \{r_{1 \leq n \leq N}\}|_{t=i\Delta t}\right). \tag{1}$$

Thus, N difference versions form a linear equation set of $\{r_i(t + \Delta t); 1 \leq i \leq N\}$ whose solutions involve inevitably in a $N \times N$ matrix. The larger N is, the more hopeless exact solution is. It is well-known that, even for a matrix algebra equation with N~tens, solving it via computer, whose kernel is an integrated circuit with GHz-level clock frequency, is a formidable task. Likewise, the time-cost of computer solving a matrix algebra equation with a N~astronomical-figure is also an astronomical-figure in units of seconds.

The AUA avoids time-consuming solving matrix equation in every time step and represents a relation differing from Equation (1)

$$r_m([i+1]\Delta t) = F\left(\{r_{1 \leq n \leq N}\}|_{t=i\Delta t}\right), \tag{2}$$

which corresponds to a diagonal matrix linking $(r_1, \cdot, r_i, \cdot, r_N)|_{t+\Delta t}$ and $(r_1, \cdot, r_i, \cdot, r_N)|_t$. Clearly, the AUA is a "non-synchronous" trick, and disagrees with the basic principle of calculation mathematics, which requires all coupled difference equations to be solved simultaneously or synchronously. Therefore, our multiple-body dynamics simulation is on a stricter route [46,47].

Our simulation is to treat N RNEs and four MEs in a non-exhaustive manner. No matter how large N is, N particles' RNEs are all Lagrangian versions of the fluid RNE of the combination of a mono-valued field $u(r, t)$ and a multiple-valued field $RV(r, t)$ [46,47]

$$u(r, t) \equiv \frac{\sum_i [d_t r_i \times \delta(r - r_i(t))]}{\sum_i \delta(r - r_i(t))}; \tag{3}$$

$$RV(r_j, t) \equiv \frac{\sum_i \left[(d_t r_j - d_t r_i) \times \delta(r_j(t) - r_i(t)) \right]}{\sum_i \delta(r_j(t) - r_i(t))}. \tag{4}$$

The phrase "mono-valued" refers to that at each space-time point (r, t), the field-value is certain. The phrase "multiple-valued" refers to otherwise cases and hence means that at each space-time point (r, t), the field-value is allowed to be over a range with a breadth. Moreover, at each space-time point (r, t), the range of allowed values of the RV-field is from the negative to the positive, and the summation of these allowed values is 0. Due to these properties, it is unnecessary to solve N RNEs and four MEs step-by-step. Instead, N particles' RNEs leads to a RNE of the mono-valued u-field, and what wait to be solved is this RNE and four MEs.

This result can also be automatically derived from the Vlasov–Maxwell description of plasmas because the solution of microscopic distribution function f should meet a physical constraint $f \geq 0$ [46]. A power series expression

$$f = \sum_{i \geq 0} c_i(r, t) [p(v) - p(u)]^i = b_0 \times \delta(v - u) + \sum_{i \geq 1} b_i(r, t) [p(v) - p(u)]^i \times (1 - \delta(v - u)), \tag{5}$$

where b_i, c_i and $u \equiv \frac{\int v f d^3 v}{\int f d^3 v}$ are functions of space-time coordinates (r, t) and $p(v) = \frac{v}{\sqrt{1 - v \cdot v}}$, can also lead to a feasible scheme of calculating f in terms of those b_i. The constraint $f \geq 0$ determines an important property of the coefficient function set $\{b_i\}$. That is, $b_1 \equiv 0$ must be fulfilled for avoiding possible presence of $f < 0$-region around $v = u$-surface within the 6D phase space.

Although an electron bunch has its own self-fields, its global motion is only affected by external fields and such self-fields affect relative motions of parts of the bunch to its "mass-center" which is defined as the zero-value point of the self-fields [47]. Namely, the self-field is responsible for the variation in the shape of the density profile of a bunch. For a bunch with considerable total charge $-Qe$, obvious global oscillation of its "mass-center" means a bright light source relative to a far-field observer.

Due to the self-fields of bunch electrons, the radiation spectrum cannot be monocolor and instead of a breadth. However, if the center of a spectrum of a breadth is at the X-ray band or higher and the breadth of the spectrum is finite, such a not-too-much-broad spectrum is of application value. After all, it is very desirable than a broad spectrum starting from an optics-frequency (OF) fundamental frequency component to a component with tens-fold frequency and relative strengths of these components decreases with respect to the harmonics order.

If viewing the behavior of each electron to be governed by the combination of the external fields and the bunch self-fields, its acceleration rate's Fourier spectrum is not a Dirac function, the spectrum should be if no self-fields exist, but instead has a finite breadth and around the frequency of the external field. Thus, the superposition of those spectrums from different electrons will be still centered/around at the frequency of the external field. Of course, for ensuring EM energy to be mainly at the center frequency, the density of the bunch cannot be overly high. Namely, although high electronic density favors high-intensity at the center frequency, it also favors those at other frequencies. It needs a compromise between high-intensity at the center frequency and the breadth of the spectrum, they are both dependent on, in different manner, the electronic density.

The self-fields cause EM energy to distribute over components differing from the center frequency determined by the external fields. If the quantity "pulse maximum strength" is defined as the maximum of superposition of the square of vector potential components at different frequency components $I = \sum_\omega |A_\omega|^2$, it might be not, or weakly, affected by the self-fields. Definite answer should be resorted

to self-consistent calculation, which will be presented elsewhere. However, the qualitative discussions above have outlined that higher values of electronic density at the zero-value point of the self-fields are favorable to yield higher intensity at the center frequency.

The dependence of the center frequency, ω_c, of the generated pulse on D, the initial electron position in the configuration, is described by a formula [41]

$$\frac{2\pi}{\omega_c} = T_{tr} + 2\sigma M \times \left[\arcsin\left(-1 + \xi\right) - \frac{\pi}{2}\right] + 2\sigma\sqrt{2\xi - \xi^2}, \tag{6}$$

where detailed expressions of T_{tr}, σ, M and ξ can be found elsewhere [40,41]. Note that ξ is linear dependent on D.

The polarization state of the generated EM pulse is usually elliptically-polarized because of the shape of the tailored Takeuchi-orbit. Because the shape can be controlled by choosing suitable values of those parameters, the polarization state is in principle able to be controlled. Some authors who are along the route 1 [48] have achieved polarization control by controlling the ellipticity of the driving laser.

3. Conclusions

The shortage of available solid-state material with electron structure suitable to generate X-ray band EM Fourier components forces us to consider how to prepare these EM Fourier components efficiently. Is it necessary to rely on advanced band-engineering to build a man-made quantum system whose electronic structure is competent for this goal? The content above answers this question. By flexible utilization of common vacuum electron components/elements, one can achieve this goal through a direct route in which low-energy electrons bunch is manipulated to efficiently generate radiations at desired wavelength and time-duration.

References

1. Itatani, J. Controlling High Harmonic Generation with Molecular Wave Packets. *Phys. Rev. Lett.* **2005**, *94*, 123902. [CrossRef] [PubMed]
2. Camus, N. Experimental Evidence for Quantum Tunneling Time. *Phys. Rev. Lett.* **2017**, *119*, 023201. [CrossRef] [PubMed]
3. Doumy, G. Attosecond Synchronization of High-Order Harmonics from Midinfrared Drivers. *Phys. Rev. Lett.* **2009**, *102*, 093002. [CrossRef] [PubMed]
4. Mauritsson, J. Attosecond Electron Spectroscopy Using a Novel Interferometric Pump-Probe Technique. *Phys. Rev. Lett.* **2010**, *105*, 053001. [CrossRef]
5. Shivaram, N. Attosecond-Resolved Evolution of a Laser-Dressed Helium Atom: Interfering Excitation Paths and Quantum Phases. *Phys. Rev. Lett.* **2012**, *108*, 193002. [CrossRef] [PubMed]
6. Wickenhauser, M. Time Resolved Fano Resonances. *Phys. Rev. Lett.* **2005**, *94*, 023002. [CrossRef] [PubMed]
7. Xie, X.H. Attosecond-Recollision-Controlled Selective Fragmentation of Polyatomic Molecules. *Phys. Rev. Lett.* **2012**, *109*, 243001. [CrossRef] [PubMed]
8. Zhao, K. Tailoring a 67 attosecond pulse through advantageous phase-mismatch. *Opt. Lett.* **2012**, *37*, 3891–3893. [CrossRef] [PubMed]
9. Goulielmakis, E.; Schultze, M.; Hofstetter, M.; Yakovlev, V.S.; Gagnon, J.; Uiberacker, M.; Aquila, A.L.; Gullikson, E.M.; Attwood, D.T.; Kienberger, R.; et al. Single-Cycle Nonlinear Optics. *Science* **2008**, *320*, 1614–1617. [CrossRef]

10. Sansone, G.; Benedetti, E.; Calegari, F.; Vozzi, C.; Avaldi, L.; Flammini, R.; Poletto, L.; Villoresi, P.; Altucci, C.; Velotta, R.; et al. Isolated Single-Cycle Attosecond Pulses. *Science* **2006**, *314*, 443–446. [CrossRef] [PubMed]
11. Christov, I.P. Attosecond Time-Scale Intra-atomic Phase Matching of High Harmonics Generation. *Phys. Rev. Lett.* **2001**, *86*, 5458–5461. [CrossRef] [PubMed]
12. Neppl, S. Attosecond Time-Resolved Photoemission from Core and Valence States of Magnesium. *Phys. Rev. Lett.* **2012**, *109*, 087401. [CrossRef] [PubMed]
13. Kelkensberg, F. Attosecond Control in Photoionization of Hydrogen Molecules. *Phys. Rev. Lett.* **2011**, *107*, 043002. [CrossRef] [PubMed]
14. Pazourek, R.; Nagele, S.; Burgdörfer, J. Attosecond Chronoscopy of Photoemission. *Phys. Rev. Lett.* **2015**, *87*, 765–768. [CrossRef]
15. Neidel, C. Probing Time-Dependent Molecular Dipoles on the Attosecond Time Scale. *Phys. Rev. Lett.* **2013**, *111*, 033001. [CrossRef] [PubMed]
16. Znakovskaya, I. Attosecond Control of Electron Dynamics in Carbon Monoxide. *Phys. Rev. Lett.* **2009**, *103*, 103002. [CrossRef] [PubMed]
17. Gilbertson, S.; Chini, M.; Feng, X.; Khan, S.; Wu, Y.; Chang, Z. Monitoring and Controlling the Electron Dynamics in Helium with Isolated Attosecond Pulses. *Phys. Rev. Lett.* **2010**, *105*, 263003. [CrossRef] [PubMed]
18. Aseyev, S.A. Attosecond Angle-Resolved Photoelectron Spectroscopy. *Phys. Rev. Lett.* **2003**, *91*, 223902. [CrossRef]
19. Johnsson, P. Attosecond Control of Ionization by Wave-Packet Interference. *Phys. Rev. Lett.* **2007**, *99*, 233001. [CrossRef]
20. Antonov, V.A. Formation of a Single Attosecond Pulse via interaction of Resonant Radiation with a Strongly Perturbed Atomic Transition. *Phys. Rev. Lett.* **2013**, *110*, 213903. [CrossRef]
21. Nisoli, M. Compression of high-energy laser pulses below 5fs. *Opt. Lett.* **1997**, *22*, 522–524. [CrossRef] [PubMed]
22. Duhr, O. Generation of intense 8-fs pulses at 400nm. *Opt. Lett.* **1999**, *24*, 34–36. [CrossRef] [PubMed]
23. Nisoli, M. Parametric generation of high-energy 14.5-fs laser pulses at 1.5um. *Opt. Lett.* **1998**, *23*, 630–632. [CrossRef] [PubMed]
24. Durfee, C.G. Intense 8-fs pulse generation in the deep ultraviolet. *Opt. Lett.* **1999**, *24*, 697–699. [CrossRef] [PubMed]
25. Treacy, E.B. Optical Pulse compression with diffraction gratings. *IEEE J. Quantum Electron.* **1969**, *5*, 454–458. [CrossRef]
26. Martinez, O.E. 3000 times grating compressor with positive group velocity dispersion: Application to fiber compensation in 1.3–1.6 um region. *IEEE J. Quantum Electron.* **1987**, *23*, 59–64. [CrossRef]
27. Strickland, D. Compression of Amplified Chirped Optical Pulses. *Opt. Commun.* **1985**, *55*, 447–449. [CrossRef]
28. Antoine, P.; L'Huillier, A.; Lewenstein, M. Attosecond Pulse Trains Using High-Order Harmonics. *Phys. Rev. Lett.* **1996**, *77*, 1234–1237. [CrossRef] [PubMed]
29. Christov, I.P. High-Harmonic Generation of Attosecond Pulses in the "Single-Cycle" Regime. *Phys. Rev. Lett.* **1997**, *78*, 1251–1254. [CrossRef]
30. Lopez-Martens, R. Amplitude and Phase Control of Attosecond Light Pulses. *Phys. Rev. Lett.* **2005**, *94*, 033001. [CrossRef]
31. Feng, X.M. Generation of Isolated Attosecond Pulses with 20 to 28 Femtosecond Lasers. *Phys. Rev. Lett.* **2009**, *103*, 183901. [CrossRef] [PubMed]
32. Takahashi, E.J. Infrared Two-Color Multicycle Laser Field Synthesis for Generating an Intense Attosecond Pulses. *Phys. Rev. Lett.* **2010**, *104*, 233901. [CrossRef]
33. Lan, P.F. Single attosecond pulse generation from asymmetric molecules with a multicycle laser pulse. *Opt. Lett.* **2007**, *32*, 1186–1188. [CrossRef] [PubMed]
34. Heissler, P. Few-Cycle Driven Relativistically Oscillating Plasma Mirrors: A Source of Intense Isolated Attosecond Pulses. *Phys. Rev. Lett.* **2012**, *108*, 235003. [CrossRef] [PubMed]
35. Behmke, M. Controlling the Spacing of Attosecond Pulse Trains from Relativistic Surface Plasmas. *Phys. Rev. Lett.* **2011**, *106*, 185002. [CrossRef] [PubMed]
36. Part, E. Simple Method to Generate Terawatt-Attosecond X-Ray Free-Electron-Laser Pulses. *Phys. Rev. Lett.* **2015**, *114*, 244801.

37. Zholentz, A.A. Proposal for Intense Attosecond Radiation from an X-Ray Free-Electron Laser. *Phys. Rev. Lett.* **2004**, *92*, 224801. [CrossRef]

38. Mikhailova, J.M. Isolated Attosecond Pulses from Laser-Driven Synchrotron Radiation. *Phys. Rev. Lett.* **2012**, *109*, 245005. [CrossRef]

39. Protopapas, M. Atomic physics with super-high intensity lasers. *Rep. Prog. Phys.* **1997**, *60*, 389–486. [CrossRef]

40. Lin, H. Monocolor Radiation Source Based on Low-energy Electron Beam and DC Fields with High Gradient of Electromagnetic Energy Density. *J. Laser Opt. Photonics* **2017**, *4*, 1000161.

41. Lin, H. A Simple and Universal setup of quasimonocolor gamma ray source. *arXiv* **2015**, arXiv:1503.00815.

42. Takeuchi, S. Relativistic $E \times B$ acceleration. *Phys. Rev. E* **2002**, *66*, 037402. [CrossRef]

43. Lin, H. Miniaturization of solid-state accelerator by compact low-energy-loss electron reflecting mirror. *EuroPhys. Lett.* **2015**, *109*, 54004. [CrossRef]

44. Dawson, J.M. Particle Simulation of Plasmas. *Rev. Mod. Phys.* **1983**, *55*, 403. [CrossRef]

45. Birdsall, C.K.; Langdon, A.B. *Plasma Physics via Computer Simulation*; Taylor and Francis Group: Didcot, UK, 2004.

46. Lin, H. Plasma Simulation beyond Rigid-Macroparticle Approximation. *J. Mod. Phys.* **2018**, *9*, 807–815. [CrossRef]

47. Lin, H. Phase space dynamics of relativistic particles. In *Accelerator Physics*; Ishaq, A., Malik, M., Eds.; Intechopen: London, UK, 2018; Chapter 1, ISBN 978-953-51-3836-5. [CrossRef]

48. Huang, P.C. Ploarization control of isolated high-harmonic pulses. *Nat. Photonics* **2018**, *12*, 349–354. [CrossRef]